

1 **Tracing historical changes, degradation, and original sources of airborne**
2 **polycyclic aromatic hydrocarbons (PAHs) in Jilin Province, China, by Abies**
3 **holophylla and Pinus tabuliformis needle leaves**

4 Zhao Wang^a, Xiangzi Jin^a, Han Yeong Kaw^b, Zakia Fatima^a, Maurizio Quinto^{a,c}, John
5 L.Zhou^d, Dongri Jin^{a,**}, Meiyu Cui^a, Donghao Li^{a,*}

6
7 ^a Department of Chemistry, Yanbian University, Park Road 977, Yanji City, Jilin Province,
8 133002, PR China

9 ^b Department of Environmental Science, Zhejiang University, Hangzhou, 310058, PR China.

10 ^c DAFNE - Department of Agriculture, Food, Natural Resources and Engineering, University
11 of Foggia, via Napoli 25, I-71122 Foggia, Italy.

12 ^d Centre for Green Technology, School of Civil and Environmental Engineering, University of
13 Technology Sydney, 15 Broadway, NSW, 2007, Australia.

14
15 ^{*}Corresponding author.

16 ^{**}Co-corresponding author.

17 E-mail addresses: dhli@ybu.edu.cn (D. Li); drjin@yby.edu.cn (D. Jin); Department of
18 Chemistry, Yanbian University, Park Road 977, Yanji City, Jilin Province, 133002, PR China.

22 **Abstract:**

23 Due to their wide distribution and availability, plant leaves are interesting biomonitoring
24 candidates for the evaluation of atmospheric pollution. In addition, leaves from some species
25 can also retain historical information, for example related to environmental pollution, due to
26 their class age. In this study, the content of polycyclic aromatic hydrocarbons (PAHs) in *Abies*
27 *holophylla* and *Pinus tabuliformis* needles in function of their class age have been investigated
28 to obtain information regarding the degradation constant for each PAH under investigation, and
29 to evaluate the possibility to correlate the presence of PAHs in needles with some important
30 environmental factors. It has been demonstrated that the total PAH concentration in the needles,
31 for both species, increased proportionally with the age of needles, ranging from 804 to 3604 ng
32 g⁻¹ (dry weight), showing a general tendency to accumulate these substances through years,
33 while degradation rates increased with molecular complexity. Finally, a study on the possible
34 correlation between adsorbed PAH contents in needle leaves and pollution emission sources
35 have been carried out, demonstrating that this biomonitoring system could be fruitfully used to
36 trace historical changes and original sources of airborne PAHs.

37 **Keywords:** Polycyclic aromatic hydrocarbons (PAHs); Air pollution biomonitoring; PAH
38 degradation constants; *Abies holophylla*; *Pinus tabuliformis*

39

40

41

42

43

44

45

46 **1. Introduction**

47 The determination of polycyclic aromatic hydrocarbons (PAHs) level caused by air
48 pollution is one of the problems of major concern in recent decades. Airborne PAHs are
49 produced by incomplete combustion of industrial emissions and transportation (Chang et al.,
50 2006; Rodgman et al., 2000), as well as wildfire (Choi, 2014; Lao et al., 2018), and their
51 monitoring has been considered a challenging and important activity, due to the carcinogenic,
52 mutagenic, and teratogenic effects of these substances on human health. PAHs determination
53 anyway could encounter technical, physical, and economical limitations when active air
54 samplers are used, while sampling tree components like needles, leaves and barks, suitable for
55 the determination of the spatial distribution of PAHs, are usually employed only to measure the
56 current levels of atmospheric PAHs (Amigo et al., 2011; De Nicola et al., 2011; Zhou et al.,
57 2014). Recent studies on the historical record of PAHs have been conducted in the growth rings,
58 lake sediments and ice cores of specific areas (Cai et al., 2016; Kuang et al., 2015; Wang et al.,
59 2008), but these sampling sites impose several constrains, limiting the monitoring to specific
60 conditions in terms of spatial recognition and time intervals.

61 Plants can be considered a very interesting and advantageous biomonitoring substrate in
62 particular for PAHs, due to the hydrophobic lipid layers that can retain these substances (Kim
63 et al., 2014; Paterson et al., 1991). For example, it has been demonstrated that diffusive uptake
64 and storage function of polymeric lipids of plants play a key role in the transport and fate of
65 phenanthrene (Li and Chen, 2014). A unique and very useful characteristic of conifer needles
66 is that they can grow up and last for several years, thus preserving the history of the
67 environmental conditions. Furthermore, some PAHs can be used as a marker of certain pollution
68 sources: for example, it was found that the prevalence of lower molecular weight compounds
69 in ambient air samples can be essentially related to the road traffic, more specifically with
70 vehicles of diesel engines (Albuquerque et al., 2016). There have also been variation studies
71 using some specific PAH content ratio in needles, such as Ant/(Ant + Phen) or Flt/(Flt + Pyr),
72 to identify local sources of contamination (Esen et al., 2008; Galarneau, 2008; Kong et al.,

73 2015).

74 On the base of these considerations, *Abies holophylla* needles from 1 to 6 years old (2016-
75 2011) old and *Pinus tabuliformis* from 1 to 4 years old (2015-2012) have been collected to
76 investigate the species-specificity historical variations of PAHs and to investigate the possible
77 relation between emitted air pollutants and PAHs in the needles over the years, also taking into
78 account the PAH degradation into the needle leaves. To pursue this target a mathematical model
79 to interpret the PAH degradation has been proposed. Finally, PAHs content in conifer needles
80 were correlated with pollutant sources of airborne PAHs throughout the studied years.

81 **2. Material and methods**

82 **2.1 Materials and standards**

83 Standard mixtures of 16 PAHs (naphthalene (Naph), acenaphthylene (Acy), acenaphthene
84 (Ace), fluorene (Fluo), phenanthrene (Phen), anthracene (Ant), fluoranthene (Flt), pyrene (Pyr),
85 benzo[a]anthracene (BaA), chrysene (Chry), benzo[b]fluoranthene (BbF),
86 benzo[k]fluoranthene (BkF), benzo[a]pyrene (BaP), indeno[1,2,3-cd] pyrene (IcdP),
87 dibenzo[a,h]anthracene (DahA) and benzo[ghi]perylene (BghiP)) and 3 deuterated PAHs
88 (Phenanthrene-d₈, Fluoranthene-d₁₂ and Perylene-d₁₂) were purchased from Sigma Aldrich (St.
89 Louis, MO, USA). The purity of all standards was up to 98%. Silica (100-200 mesh) and Al₂O₃
90 adsorbent was obtained from Sigma Aldrich (St. Louis, MO, USA). To remove the
91 contaminants, all adsorbents and glasswares were heated at 400°C for 12 h.

92 **2.2 Sampling and processing**

93 Two plant species with 4 years and 6 years old needles were selected for this study. Needles
94 from 1 (2016) to 6 years (2011) and from 1 (2015) to 4 years (2012) old were collected from
95 *Abies holophylla* and *Pinus tabuliformis*, respectively. Age of needles was evaluated by growth
96 ring and branching pattern, and it was confirmed in combination with the situation at the branch
97 cut (**Fig. 1**) (Pérez-Harguindeguy et al., 2013). During collection, in order to ensure a better

98 authenticity and accuracy, needles of the same year at the upper 1/3 and lower 1/3 of the canopy
99 of tree species were mixed into one sample, cleaned, freeze-dried, crushed by 200 mesh, and
100 stored at -20°C for further analysis.



101
102 **Fig. 1.** Photographs that show the branch information of A) *Abies holophylla*, and the growth
103 ring patterns of B) *Abies holophylla* and C) *Pinus tabuliformis*.

104 Eleven air pollutant emission variables with an expected environmental impact on the
105 concentrations of PAHs, namely coal (Ton year⁻¹), crude oil (Ton year⁻¹), and electricity (MKh
106 year⁻¹) consumption; number of civil vehicles and trucks (Unit year⁻¹); emission of industrial
107 sulfur, nitrogen oxide, industrial smoke (dust), and soot (Ton year⁻¹); urban living gaseous
108 pollutant emissions (Ton year⁻¹); generating capacity (KWh year⁻¹) were obtained for the
109 interested areas from the databases of the China National Statistics Institute (“SBJ (Statistic
110 bureau of Jilin-Statistics China),” 2016).

111 **2.3 Measurement of lipid content**

112 Needle lipid contents were measured as follows: 3 g of dry needles were extracted 3 times
113 using ultrasonication with 20 mL n-hexane:acetone (50:50, v:v) for 20 min each. The extract
114 was concentrated, dried and finally weighed to calculate the lipid content (Zhao et al., 2018).

2.4 PAHs analysis

2.4.1 Extraction of PAHs

All the samples were spiked using internal standards. The sample pre-treatment procedures were performed according to the method in our previous publication with slight modification (Jin et al., 2020). In brief, a total of 0.5 g homogenized, crushed and sieved needles powder was spiked with internal standards, then mixed with 10 mL of dichloromethane (DCM) and ultrasonically extracted 3 times per 15 min. The combined extract was replaced with n-hexane and concentrated to 0.5 mL prior to SPE clean up. The SPE column (down-top: 2.0 g Na₂SO₄, 1.5 g silica gel, 0.8 g Al₂O₃ (deactivated with 2% ultrapure water), and 4.0 g Na₂SO₄) was conditioned with n-hexane before sample loading. It was eluted with 3 mL n-hexane (discarded) followed by 9 mL n-hexane/DCM (1:1, v/v) (first 3 mL was discarded). The 6 mL eluted extract was concentrated via a gentle stream of nitrogen gas at room temperature, and reconstituted with 100 μL of n-hexane. Then, gas purge microsyringe extraction (GP-MSE) was used for further purification, as described in a previous work (Yang et al., 2011), and the final volume was adjusted to 100 μL. Finally, 2 μL of the purified extract was injected to the GC-MS system for analysis.

2.4.2 GC-MS analysis

PAHs were analyzed quantitatively and qualitatively by Shimadzu gas chromatograph equipped with DB-5MS fused silica capillary column (30 m × 0.25 mm; thickness: 0.25 μm, Restek Corporation, Bellefonte, PA, USA) and QPMS 2010 mass spectrometry detector. The conditions for GC-MS analysis were as follows: sample injection was carried out in splitless mode at 280°C, using He as a carrier gas at a flow rate of 1 ml min⁻¹. GC-MS interface temperature was set at 280°C, ionization voltage was 70 eV and ion source temperature was set at 200°C. The initial oven temperature was held at 80°C for 1 min, then was brought to 100°C at the rate of 20°C min⁻¹, from 100°C to 200°C at 10°C min⁻¹ and 200°C to 280°C at 20°C min⁻¹, holding this last value for 2 min. Data was collected in selected ion monitoring mode (SIM).

141 The relative percentage difference for individual PAH determined in paired duplicate samples
 142 ($n = 2$) was always $< 24\%$. The obtained recovery for all the PAHs was between 64 and 120%
 143 with respect to the certified values.

144 3. Results and discussion

145 3.1 Adsorbed PAHs in needles

146 Usually, PAHs content in plant samples is normalized by lipid content or dry weight.
 147 Studies have shown that both cuticle and suberin (a cell wall component) may act as lipids in
 148 different parts of the plant, but they are not solvent extractable (Chen et al., 2012; Ockenden et
 149 al., 1998; Taiz and Zeiger, 2010). For this reason, the needle lipid content obtained by the
 150 classical method may not reflect the total amount of substances acting as PAH extracting lipids.
 151 The total measured extractable PAH concentrations found in this work are given in **Table 1**.
 152 The needle lipid contents in *Abies holophylla* and *Pinus tabuliformis* ranged from 27.46 to
 153 32.16%, and from 6.85 to 9.56% (respect to dry weight), respectively. By comparing the total
 154 extractable PAH concentrations with lipid contents of needles, no significant correlation was
 155 found ($R = -0.12 - 0.646$, $p > 0.354$). Hence PAHs contents were expressed on a dry weight
 156 basis in this study.

157 **Table 1** Temporal trends of PAH total contents recorded in needles of *Abies holophylla* and
 158 *Pinus tabuliformis*.

Rings	<i>Abies holophylla</i> (ng g ⁻¹)					
	2016	2015	2014	2013	2012	2011
2	43 ± 2	52 ± 17	42 ± 5	38 ± 1	38 ± 2	45 ± 7
3	981 ± 76	1503 ± 10	1669 ± 13	1820 ± 82	2135 ± 149	2340 ± 34
4	438 ± 133	588 ± 98	762 ± 204	815 ± 158	893 ± 84	1228 ± 130
5,6	18 ± 1	14 ± 1	9 ± 2	16 ± 2	10 ± 4	21 ± 7
Total PAHs	1449 ± 212	2113 ± 106	2446 ± 189	2663 ± 73	3044 ± 67	3604 ± 96

159

Rings	<i>Pinus tabuliformis</i> (ng g ⁻¹)			
	2015	2014	2013	2012

2	119 ± 4	100 ± 1	105 ± 25	72 ± 8
3	498 ± 112	829 ± 102	845 ± 66	910 ± 39
4	152 ± 10	241 ± 22	319 ± 51	308 ± 30
5,6	34 ± 7	28 ± 3	65 ± 39	145 ± 77
Total PAHs	804 ± 99	1197 ± 127	1334 ± 131	1435 ± 93

160 As expected, due to the accumulating effect, PAH contents generally increase with the
161 needles age, accordingly to the results obtained by previous works (Odabasi et al., 2015; Ratola
162 et al., 2010a). Furthermore, *Abies holophylla* needles generally showed a higher tendency to
163 accumulate PAHs in respect to *Pinus tabuliformis* needles. The concentration of 3-4 ring PAHs
164 increase over time, and this result is consistent with a previous work (Ratola et al., 2010a).
165 These values were found to be higher than 5-6 ring PAHs, which are in good agreement with
166 the accumulation pattern of PAHs in needles of other pine species, including *Pinus halepensis*
167 and *P. pinea* (Librando et al., 2002), *Pinus pinaster* and *Pinus nigra* (Piccardo et al., 2005) and
168 *P. pinaster* and *P. pinea* (Ratola et al., 2010a). Because of the volatile nature of Naph (2 ring),
169 its fast photodegradation process and re-suspension capability leads to a non-stable
170 accumulation in the needles (Choi, 2014; Wang et al., 2005). Lighter PAHs (3-4 ring), which
171 are predominantly present in the gaseous phase, interact strongly with the waxy layer of the
172 needles and this effect can promote PAH uptakes in needles (Lehndorff and Schwark, 2004).
173 The low content of heavier PAHs (5-6 rings) observed in this work confirms what already
174 noticed in previous works, and it could be related to the fact that their adsorption in needle
175 leaves can be hindered by their different distribution in the environment. These PAHs are
176 present in fact preferentially in the particulate phase of the atmosphere, and for this reason their
177 migration from atmosphere can be slower if compared with other PAHs (Yang et al., 2017). The
178 accumulation process may vary from species to species, leading to different concentration in
179 needles (Ratola et al., 2011). This behavior has been noticed also for the species in this work,
180 even if a similar PAH trend for years 1 to 4 with *Abies holophylla* and *Pinus tabuliformis*
181 needles were noticed. More than 64 % of adsorbed PAHs in the needles are composed of 3-4
182 rings: this value roughly reflects PAH composition in the air in both urban and industrial areas
183 (Li et al., 2016; Odabasi et al., 2015; Tomashuk et al., 2012).

184 **3.2 A study on PAH degradation constants in *Abies holophylla* needles**

185 As already pointed out, PAHs are present in gas and particle phases of the atmosphere and
 186 diffuse into plant leaves through dry and wet deposition. Their sources are closely related to the
 187 anthropogenic combustion processes (e.g. car exhaust, local heating facilities, industrial related
 188 activities). It has been already demonstrated that the PAH degradation follows a first-order
 189 kinetics (Haritash and Kaushik, 2009), even if dependent from external variables: for example,
 190 fly ash and carbon black, that can protect PAHs from photo decomposition (Behymer and Hites,
 191 1985; Korfmacher et al., 1980). Anyway, in principle the PAH amount collected in different
 192 years by needles undergo through a degradation mechanism that follows an exponential trend,
 193 which can be described by these equations:

$$C_{year}^{Tot} = \sum_{i=0}^n C_i e^{-\alpha t_i} \quad \text{Eq.1}$$

194 Where C_{year}^{Tot} is the content (obtained experimentally) for each PAH, C_i is the PAH
 195 amount that can be attributed to a specific year, α is the degradation kinetic constant and t_i is
 196 the time expressed in years. This model was then applied to PAH contents in *Abies holophylla*
 197 needles, considering that for this species data were collected from 2011 to 2016, a longer period
 198 if compared to data obtained by *Pinus tabuliformis*. In this case, it is possible to write for each
 199 year the following equations:

$$C_{2011}^{Tot} = C_{\leq 2010} e^{-\alpha} + C_{2011} \quad \text{Eq.2}$$

$$C_{2012}^{Tot} = C_{\leq 2010} e^{-2\alpha} + C_{2011} e^{-\alpha} + C_{2012} \quad \text{Eq.3}$$

$$C_{2013}^{Tot} = C_{\leq 2010} e^{-3\alpha} + C_{2011} e^{-2\alpha} + C_{2012} e^{-\alpha} + C_{2013} \quad \text{Eq.4}$$

$$C_{2014}^{Tot} = C_{\leq 2010} e^{-4\alpha} + C_{2011} e^{-3\alpha} + C_{2012} e^{-2\alpha} + C_{2013} e^{-\alpha} + C_{2014} \quad \text{Eq.5}$$

$$C_{2015}^{Tot} = C_{\leq 2010} e^{-5\alpha} + C_{2011} e^{-4\alpha} + C_{2012} e^{-3\alpha} + C_{2013} e^{-2\alpha} + C_{2014} e^{-\alpha} + C_{2015} \quad \text{Eq.6}$$

$$C_{2016}^{Tot} = C_{\leq 2010} e^{-6\alpha} + C_{2011} e^{-5\alpha} + C_{2012} e^{-4\alpha} + C_{2013} e^{-3\alpha} + C_{2014} e^{-2\alpha} +$$

$$C_{2015} e^{-\alpha} + C_{2016} \quad \text{Eq.7}$$

200 Considering $e^{-at} = y$ we have:

$$C_{2011}^{Tot} = C_{\leq 2010}y + C_{2011} \quad \text{Eq.8}$$

$$C_{2012}^{Tot} = C_{\leq 2010}y^2 + C_{2011}y + C_{2012} = (C_{\leq 2010}y + C_{2011})y + C_{2012} = C_{2011}^{Tot}y + C_{2012} \quad \text{Eq.9}$$

201 and then, applying the same elaboration to other years:

$$C_{2013}^{Tot} = C_{2012}^{Tot}y + C_{2013} \quad \text{Eq.10}$$

$$C_{2014}^{Tot} = C_{2013}^{Tot}y + C_{2014} \quad \text{Eq.11}$$

$$C_{2015}^{Tot} = C_{2014}^{Tot}y + C_{2015} \quad \text{Eq.12}$$

$$C_{2016}^{Tot} = C_{2015}^{Tot}y + C_{2016} \quad \text{Eq.13}$$

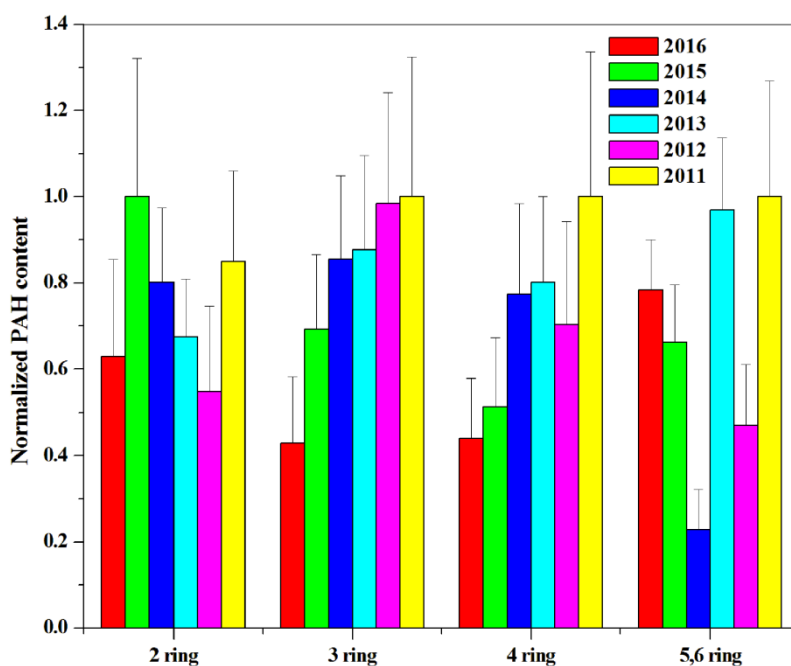
202 On the base of **Eq. 9-13**, considering that C_{year} and y should be always ≥ 0 , it is possible
 203 to individuate the minimum acceptable α values and the relevant minimum PAH degradation
 204 percentage per year (**Table 2**). To our knowledge, no studies have been carried out regarding
 205 the PAH degradation in leaves. Cutright (Cutright, 1995) reported a study to determine the
 206 specific degradation rates for the bioremediation of PAH-contaminated soils. Other studies
 207 demonstrated that the degradation rate of high molecular weight PAHs is slower than other
 208 PAHs (Johnsen et al., 2005), and as an important factor for the PAH-degradation activity, of the
 209 pH changes by the bacteria could be the reason (Kästner et al., 1998).

210 **Table 2** Minimum percentage of PAH degradation year⁻¹ and minimum values of the
 211 degradation constant.

Rings	Compound	Minimum degradation per year (%)	Minimum a value
2	Naph	32	0.387
3	Acy	16	0.173
3	Ace	34	0.421
3	Fluo	39	0.501
3	Phen	27	0.309
3	Ant	41	0.533
3	Flt	35	0.428

4	Pyr	35	0.423
4	BaA	39	0.496
4	Chry	32	0.382
4	BbF	35	0.434
4	BkF	62	0.962
4	BaP	25	0.987
5	IcdP	81	1.681
5	DahA	85	1.870
6	BghiP	81	1.647

212 On the contrary, in this study it is interesting to note that higher is the number of rings (i.e.
 213 IcdP, DahA and BghiP), higher is the degradation constant, with the consequence of high
 214 degradation rates. This different behavior is most probably due to the fact that degradation rates
 215 in soil are governed by bacteria activity (Roslund et al., 2018), which is not present in the
 216 needles where decomposition is mostly dependent on PAH chemical stability. The proposed
 217 degradation model allows an estimation of the PAH contents retained by needles every year. In
 218 **Fig. 2**, the normalized PAH contents in needle are displayed. 3 and 4 rings PAHs show a
 219 decrease from 2011 to 2016, while for 2 and 5-6 rings PAHs the behavior seems not following
 220 any particular trend.



221
 222 **Fig. 2.** Normalized PAH content differentiated by the number of rings, in function of different

223 years. Error bars represent standard deviations.

224 **3.3 Correlation between adsorbed PAHs in *Abies holophylla* needles and air pollutant** 225 **emission variables in needles**

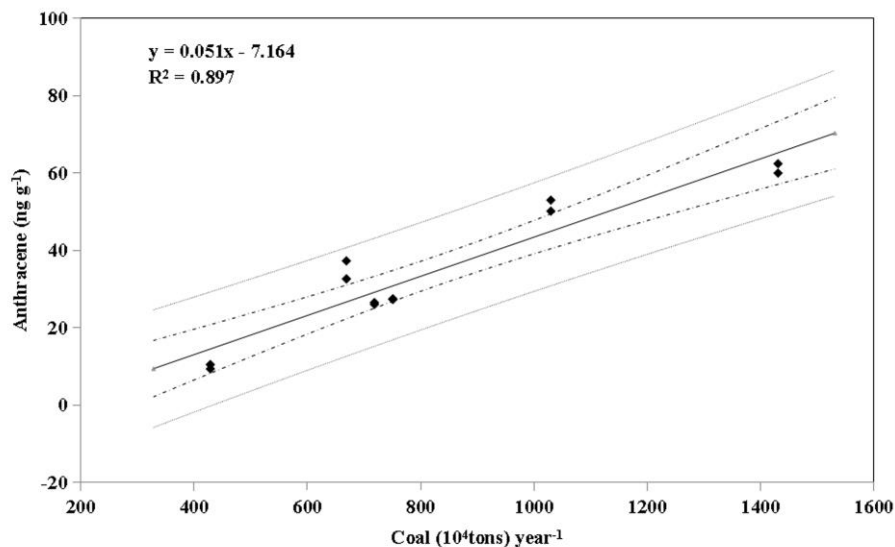
226 PAHs sources are closely related to the anthropogenic combustion processes (e.g. car
227 exhaust, local heating facilities, industrial related activities). For this reason, it could be
228 hypothesized a correlation between adsorbed PAHs and some air pollutant emission parameters.
229 From China National Statistics Institute, it is possible to obtain data concerning: annual
230 consumption of coal (Ton year⁻¹), crude oil (Ton year⁻¹) and electricity (MkWh year⁻¹)
231 consumption; number of civil vehicles and trucks (Unit year⁻¹); emission of industrial sulfur,
232 nitrogen oxide, industrial smoke (dust), and soot (Ton year⁻¹); urban living gaseous pollutant
233 emissions (Ton year⁻¹); generating capacity (KWh year⁻¹). Correlation coefficients were then
234 obtained considering these parameters and PAHs average values from *Abies holophylla*.

235 **Table 3** Correlation coefficients (R) between air pollution parameters and the average values
236 of adsorbed PAHs obtained from *Abies holophylla*. Only R > 0.8 values are displayed.

Air pollutant parameter	PAH	Correlation coefficient(R)
Coal	Fluo	0.817
	Phen	0.947
	Ant	0.874
	Flt	0.915
Electricity	Pyr	0.925
	BaA	0.906
	Chry	0.947
Trucks	BbF	0.814
Industrial sulfur emissions	Fluo	0.862
	Phen	0.857
	Acy	0.869
	Ace	0.982
Industrial nitrogen oxide emissions	Fluo	0.956
	Phen	0.934
	Ant	0.848
	Flt	0.908

	Pyr	0.833
Vehicle number	BaP	0.888
	Ace	0.816
Industrial gaseous pollutant emissions	Fluo	0.866
	Phen	0.864
	Flt	0.915
Generating capacity	Pyr	0.925
	BaA	0.911
	Chry	0.947

237 The concentration of PAH congener shows good correlation with meteorological
238 parameters (**Table 3**). For example, **Fig. 3** shows a typical correlation graph obtained between
239 coal consumption per year and Ant contents in needle. Several interesting considerations can
240 be made based on Table 3. For instance, Fluo, Phen and Ant are well correlated with coal
241 consumption, and this correlation can be ascribed to their production during combustion
242 (Dameng et al., 2011). In particular, in this last process, Phen production is the highest when
243 compared to the PAHs investigated in this work, and this could lead to the very high correlation
244 value (0.947). On the other hand, these three PAHs are not the only ones produced during coal
245 combustion, but, most probably, the lack in correlation could be due to other interfering
246 processes. The correlation existing between the number of trucks and BbF can be ascribed to
247 its production by diesel engines (Kuusimäki et al., 2002). It is also worth to note the high
248 number of PAH that are correlated with industrial nitrogen oxide emissions, suggesting that
249 NOx production can be strongly related to the emission of these PAHs in the atmosphere.



250

251 **Fig. 3.** A graph showing the correlations between coal consumption per year and anthracene
 252 content in *Abies holophylla* leaves. The solid line and dotted line curves represent
 253 confidence limits for the prediction and confidence limits for the regression line at
 254 95% confidence level, respectively.

255 In the urban areas, traffic emission is the dominant source of PAHs (Ratola et al., 2010b),
 256 in particular 3-4 rings PAHs: this could explain the good correlation between vehicle number
 257 and BaP. Surprisingly, none of the 5 and 6 ring PAHs shows correlation with any of the pollution
 258 sources, probably because of their fast degradation constant ($\alpha \geq 1.65$) that does not allow to
 259 recover time dependent information from needles, and due to the molecule dimensions that
 260 make it more difficult to be adsorbed onto pine needles (Yang et al., 2007).

261 4. Conclusions

262 In this study, the possibility to evaluate PAH historical changes and their correlation with
 263 pollution emission sources by PAH contents in the needles of *Abies holophylla* and *Pinus*
 264 *tabuliformis* has been investigated. Using the PAH content in *Abies holophylla* needles, a
 265 mathematical model that consider a first order PAH degradation process has been applied in
 266 order to obtain the minimum degradation per year and the minimum α value for each of the
 267 considered PAH. Results indicate that higher is the number of rings (i.e. IcdP and DahA and

268 BghiP), higher is the degradation constant in the needles, with the consequence of high
269 degradation rates. Furthermore, considering that PAHs sources are closely related to the
270 anthropogenic pollution processes, the adsorbed PAHs content calculated by the mathematical
271 model from 2011 to 2016 in *Abies holophylla* leaves have been statistically compared with air
272 pollutant emission parameters obtained from the databases, obtaining in some cases a good
273 correlation ($R > 0.8$) among data. The obtained results indicate that adsorbed PAHs in needle
274 leaves are good candidate as biomonitoring system to evaluate the historical changes of PAHs
275 induced by pollutant emission on the regional scale.

276

277 **Conflicts of interest**

278 The authors declare that they have no known competing financial interests or personal
279 relationships that could have appeared to influence the work reported in this paper.

280

281 **Acknowledgement**

282 This study was supported by a grant from the National Natural Science Foundation of
283 China (No. 413010201) and the 111 Project (D18012).

284

285 **References**

- 286 Albuquerque, M., Coutinho, M., Borrego, C., 2016. Long-term monitoring and seasonal
287 analysis of polycyclic aromatic hydrocarbons (PAHs) measured over a decade in the
288 ambient air of Porto, Portugal. *Science of The Total Environment* 543, 439–448.
289 <https://doi.org/10.1016/j.scitotenv.2015.11.064>
- 290 Amigo, J.M., Ratola, N., Alves, A., 2011. Study of geographical trends of polycyclic aromatic
291 hydrocarbons using pine needles. *Atmospheric Environment* 45, 5988–5996.
292 <https://doi.org/10.1016/j.atmosenv.2011.07.058>
- 293 Cai, Y., Wang, X., Wu, Y., Li, Y., Ya, M., 2016. Over 100-year sedimentary record of polycyclic
294 aromatic hydrocarbons (PAHs) and organochlorine compounds (OCs) in the continental
295 shelf of the East China Sea. *Environmental Pollution* 219, 774–784.
296 <https://doi.org/10.1016/j.envpol.2016.07.053>
- 297 Chang, K.-F., Fang, G.-C., Chen, J.-C., Wu, Y.-S., 2006. Atmospheric polycyclic aromatic
298 hydrocarbons (PAHs) in Asia: A review from 1999 to 2004. *Environmental Pollution*
299 142, 388–396. <https://doi.org/10.1016/j.envpol.2005.09.025>
- 300 Chen, P., Mei, J., Peng, P., Hu, J., Chen, D., 2012. Atmospheric PCDD/F Concentrations in 38
301 Cities of China Monitored with Pine Needles, a Passive Biosampler. *Environmental*
302 *Science & Technology* 46, 13334–13343. <https://doi.org/10.1021/es303468y>
- 303 Choi, S.-D., 2014. Time trends in the levels and patterns of polycyclic aromatic hydrocarbons
304 (PAHs) in pine bark, litter, and soil after a forest fire. *Science of The Total Environment*
305 470–471, 1441–1449. <https://doi.org/10.1016/j.scitotenv.2013.07.100>
- 306 Cutright, T.J., 1995. Polycyclic aromatic hydrocarbon biodegradation and kinetics using
307 *Cunninghamella echinulata* var. *elegans*. *International Biodeterioration &*
308 *Biodegradation* 35, 397–408. [https://doi.org/10.1016/0964-8305\(95\)00046-1](https://doi.org/10.1016/0964-8305(95)00046-1)
- 309 Dameng, L., Zhihua, L., Yunyong, L., 2011. Distribution and Occurrence of Polycyclic

310 Aromatic Hydrocarbons from Coal Combustion and Coking and its Impact on the
311 Environment. Energy Procedia 5, 734–741.
312 <https://doi.org/10.1016/j.egypro.2011.03.129>

313 De Nicola, F., Claudia, L., Maria Vittoria, P., Giulia, M., Anna, A., 2011. Biomonitoring of PAHs
314 by using *Quercus ilex* leaves: Source diagnostic and toxicity assessment. Atmospheric
315 Environment 45, 1428–1433. <https://doi.org/10.1016/j.atmosenv.2010.12.022>

316 Esen, F., Tasdemir, Y., Vardar, N., 2008. Atmospheric concentrations of PAHs, their possible
317 sources and gas-to-particle partitioning at a residential site of Bursa, Turkey.
318 Atmospheric Research 88, 243–255. <https://doi.org/10.1016/j.atmosres.2007.11.022>

319 Galarneau, E., 2008. Source specificity and atmospheric processing of airborne PAHs:
320 Implications for source apportionment. Atmospheric Environment 42, 8139–8149.
321 <https://doi.org/10.1016/j.atmosenv.2008.07.025>

322 Haritash, A.K., Kaushik, C.P., 2009. Biodegradation aspects of Polycyclic Aromatic
323 Hydrocarbons (PAHs): A review. Journal of Hazardous Materials 169, 1–15.
324 <https://doi.org/10.1016/j.jhazmat.2009.03.137>

325 Johnsen, A.R., Wick, L.Y., Harms, H., 2005. Principles of microbial PAH-degradation in soil.
326 Environmental Pollution 133, 71–84. <https://doi.org/10.1016/j.envpol.2004.04.015>

327 Jin, X., Kaw, H.Y., Li, H., Wang, Z., Zhao, J., Piao, X., Li, D., Jin, D., He, M., 2020. A traceless
328 clean-up method coupled with gas chromatography and mass spectrometry for
329 analyzing polycyclic aromatic hydrocarbons in complex plant leaf matrices. The
330 Analyst 145, 3266–3273. <https://doi.org/10.1039/D0AN00128G>

331 Kästner, M., Breuer-Jammali, M., Mahro, B., 1998. Impact of Inoculation Protocols, Salinity,
332 and pH on the Degradation of Polycyclic Aromatic Hydrocarbons (PAHs) and Survival
333 of PAH-Degrading Bacteria Introduced into Soil. Appl. Environ. Microbiol. 64, 359–
334 362. <https://doi.org/10.1128/AEM.64.1.359-362.1998>

- 335 Kim, S.-J., Lee, H., Kwon, J.-H., 2014. Measurement of partition coefficients for selected
336 polycyclic aromatic hydrocarbons between isolated plant cuticles and water. *Science of*
337 *The Total Environment* 494–495, 113–118.
338 <https://doi.org/10.1016/j.scitotenv.2014.06.119>
- 339 Kong, S., Li, X., Li, L., Yin, Y., Chen, K., Yuan, L., Zhang, Y., Shan, Y., Ji, Y., 2015. Variation
340 of polycyclic aromatic hydrocarbons in atmospheric PM_{2.5} during winter haze period
341 around 2014 Chinese Spring Festival at Nanjing: Insights of source changes, air mass
342 direction and firework particle injection. *Science of The Total Environment* 520, 59–72.
343 <https://doi.org/10.1016/j.scitotenv.2015.03.001>
- 344 Kuang, Y., Li, J., Hou, E., 2015. Lipid-content-normalized polycyclic aromatic hydrocarbons
345 (PAHs) in the xylem of conifers can indicate historical changes in regional airborne
346 PAHs. *Environmental Pollution* 196, 53–59.
347 <https://doi.org/10.1016/j.envpol.2014.09.018>
- 348 Kuusimäki, L., Peltonen, Y., Kyyrö, E., Mutanen, P., Peltonen, K., Savela, K., 2002. Exposure
349 of garbage truck drivers and maintenance personnel at a waste handling centre to
350 polycyclic aromatic hydrocarbons derived from diesel exhaust. *J. Environ. Monit.* 4,
351 722–727. <https://doi.org/10.1039/B203443N>
- 352 Lao, J.-Y., Xie, S.-Y., Wu, C.-C., Bao, L.-J., Tao, S., Zeng, E.Y., 2018. Importance of Dermal
353 Absorption of Polycyclic Aromatic Hydrocarbons Derived from Barbecue Fumes.
354 *Environ. Sci. Technol.* 52, 8330–8338. <https://doi.org/10.1021/acs.est.8b01689>
- 355 Lehndorff, E., Schwark, L., 2004. Biomonitoring of air quality in the Cologne Conurbation
356 using pine needles as a passive sampler—Part II: polycyclic aromatic hydrocarbons
357 (PAH). *Atmospheric Environment* 38, 3793–3808.
358 <https://doi.org/10.1016/j.atmosenv.2004.03.065>
- 359 Li, Q., Chen, B., 2014. Organic Pollutant Clustered in the Plant Cuticular Membranes:

360 Visualizing the Distribution of Phenanthrene in Leaf Cuticle Using Two-Photon
361 Confocal Scanning Laser Microscopy. *Environ. Sci. Technol.* 48, 4774–4781.
362 <https://doi.org/10.1021/es404976c>

363 Li, X., Yang, Y., Xu, X., Xu, C., Hong, J., 2016. Air pollution from polycyclic aromatic
364 hydrocarbons generated by human activities and their health effects in China. *Journal*
365 *of Cleaner Production* 112, 1360–1367. <https://doi.org/10.1016/j.jclepro.2015.05.077>

366 Librando, V., Perrini, G., Tomasello, M., 2002. Biomonitoring of Atmospheric PAHs by
367 Evergreen Plants: Correlations and Applicability. *Polycyclic Aromatic Compounds* 22,
368 549–559. <https://doi.org/10.1080/10406630290103726>

369 Ockenden, W.A., Steinnes, E., Parker, C., Jones, K.C., 1998. Observations on Persistent
370 Organic Pollutants in Plants: Implications for Their Use as Passive Air Samplers and for
371 POP Cycling. *Environ. Sci. Technol.* 32, 2721–2726. <https://doi.org/10.1021/es980150y>

372 Odabasi, M., Ozgunerge Falay, E., Tuna, G., Altioek, H., Kara, M., Dumanoglu, Y., Bayram, A.,
373 Tolunay, D., Elbir, T., 2015. Biomonitoring the Spatial and Historical Variations of
374 Persistent Organic Pollutants (POPs) in an Industrial Region. *Environmental Science &*
375 *Technology* 49, 2105–2114. <https://doi.org/10.1021/es506316t>

376 Paterson, S., Mackay, D., Bacci, E., Calamari, D., 1991. Correlation of the equilibrium and
377 kinetics of leaf-air exchange of hydrophobic organic chemicals. *Environ. Sci. Technol.*
378 25, 866–871. <https://doi.org/10.1021/es00017a006>

379 Pérez-Harguindeguy, N., Díaz, S., Garnier, E., Lavorel, S., Poorter, H., Jaureguiberry, P., Bret-
380 Harte, M.S., Cornwell, W.K., Craine, J.M., Gurvich, D.E., Urcelay, C., Veneklaas, E.J.,
381 Reich, P.B., Poorter, L., Wright, I.J., Ray, P., Enrico, L., Pausas, J.G., de Vos, A.C.,
382 Buchmann, N., Funes, G., Quétier, F., Hodgson, J.G., Thompson, K., Morgan, H.D., ter
383 Steege, H., Sack, L., Blonder, B., Poschlod, P., Vaieretti, M.V., Conti, G., Staver, A.C.,
384 Aquino, S., Cornelissen, J.H.C., 2013. New handbook for standardised measurement of

385 plant functional traits worldwide. *Aust. J. Bot.* 61, 167.
386 <https://doi.org/10.1071/BT12225>

387 Piccardo, M.T., Pala, M., Bonaccorso, B., Stella, A., Redaelli, A., Paola, G., Valerio, F., 2005.
388 *Pinus nigra* and *Pinus pinaster* needles as passive samplers of polycyclic aromatic
389 hydrocarbons. *Environmental Pollution* 133, 293–301.
390 <https://doi.org/10.1016/j.envpol.2004.05.034>

391 Ratola, N., Amigo, J.M., Alves, A., 2010a. Comprehensive assessment of pine needles as
392 bioindicators of PAHs using multivariate analysis. The importance of temporal trends.
393 *Chemosphere* 81, 1517–1525. <https://doi.org/10.1016/j.chemosphere.2010.08.031>

394 Ratola, N., Amigo, J.M., Alves, A., 2010b. Levels and Sources of PAHs in Selected Sites from
395 Portugal: Biomonitoring with *Pinus pinea* and *Pinus pinaster* Needles. *Arch Environ*
396 *Contam Toxicol* 58, 631–647. <https://doi.org/10.1007/s00244-009-9462-0>

397 Ratola, N., Amigo, J.M., Oliveira, M.S.N., Araújo, R., Silva, J.A., Alves, A., 2011. Differences
398 between *Pinus pinea* and *Pinus pinaster* as bioindicators of polycyclic aromatic
399 hydrocarbons. *Environmental and Experimental Botany* 72, 339–347.
400 <https://doi.org/10.1016/j.envexpbot.2011.04.012>

401 Rodgman, A., Smith, C.J., Perfetti, T.A., 2000. The composition of cigarette smoke: a
402 retrospective, with emphasis on polycyclic components. *Hum Exp Toxicol* 19, 573–595.
403 <https://doi.org/10.1191/096032700701546514>

404 SBJ (Statistic bureau of Jilin – Statistics China) [WWW Document], 2016. URL
405 <http://tjj.jl.gov.cn/tjsj/> (accessed 7.12.20).

406 Taiz, L., Zeiger, E., 2010. *Plant physiology*, 5th ed. ed. Sinauer Associates, Sunderland, MA.

407 Tomashuk, T.A., Truong, T.M., Mantha, M., McGowin, A.E., 2012. Atmospheric polycyclic
408 aromatic hydrocarbon profiles and sources in pine needles and particulate matter in
409 Dayton, Ohio, USA. *Atmospheric Environment* 51, 196–202.

- 410 <https://doi.org/10.1016/j.atmosenv.2012.01.028>
- 411 Wang, D., Chen, J., Xu, Z., Qiao, X., Huang, L., 2005. Disappearance of polycyclic aromatic
412 hydrocarbons sorbed on surfaces of pine [*Pinus thunbergii*] needles under irradiation of
413 sunlight: Volatilization and photolysis. *Atmospheric Environment* 39, 4583–4591.
414 <https://doi.org/10.1016/j.atmosenv.2005.04.008>
- 415 Wang, X. ping, Xu, B. qing, Kang, S. chang, Cong, Z. yuan, Yao, T. dong, 2008. The historical
416 residue trends of DDT, hexachlorocyclohexanes and polycyclic aromatic hydrocarbons
417 in an ice core from Mt. Everest, central Himalayas, China. *Atmospheric Environment*
418 42, 6699–6709. <https://doi.org/10.1016/j.atmosenv.2008.04.035>
- 419 Yang, B., Liu, S., Liu, Y., Li, X., Lin, X., Liu, M., Liu, X., 2017. PAHs uptake and translocation
420 in *Cinnamomum camphora* leaves from Shanghai, China. *Science of The Total*
421 *Environment* 574, 358–368. <https://doi.org/10.1016/j.scitotenv.2016.09.058>
- 422 Yang, P., Chen, J., Wang, Z., Qiao, X., Cai, X., Tian, F., Ge, L., 2007. Contributions of deposited
423 particles to pine needle polycyclic aromatic hydrocarbons. *J. Environ. Monit.* 9, 1248.
424 <https://doi.org/10.1039/b708508g>
- 425 Zhao, X., He, M., Shang, H., Yu, H., Wang, H., Li, H., Piao, J., Quinto, M., Li, D., 2018.
426 Biomonitoring polycyclic aromatic hydrocarbons by *Salix matsudana* leaves: A
427 comparison with the relevant air content and evaluation of environmental parameter
428 effects. *Atmospheric Environment* 181, 47–53.
429 <https://doi.org/10.1016/j.atmosenv.2018.03.004>
- 430 Zhou, L., Dong, L., Huang, Y., Shi, S., Zhang, L., Zhang, X., Yang, W., Li, L., 2014. Spatial
431 distribution and source apportionment of polycyclic aromatic hydrocarbons (PAHs) in
432 Camphor (*Cinnamomum camphora*) tree bark from Southern Jiangsu, China.
433 *Chemosphere* 107, 297–303. <https://doi.org/10.1016/j.chemosphere.2013.12.070>

434

Declaration of interests

The authors declare that they have no known competing financial interests or personal relationships that could have appeared to influence the work reported in this paper.

The authors declare the following financial interests/personal relationships which may be considered as potential competing interests:

Sincerely,

Donghao Li

Department of Chemistry, Yanbian University, Park Road 977, Yanji City, Jilin Province,
133002, PR China.

Tel.: +86-0433-2436456

E-mail: dhli@ybu.edu.cn



Highlights

- PAH contents in *Abies holophylla* and *Pinus tabuliformis* needles have been evaluated.
- A mathematical model to calculate PAH degradation in pine needles was developed.
- Degradation constants in needles increased with the number of rings in PAHs.
- Correlations between specific adsorbed PAHs in needle leaves and air pollutant sources was found.

Figure 1
[Click here to download high resolution image](#)



Figure 2
[Click here to download high resolution image](#)

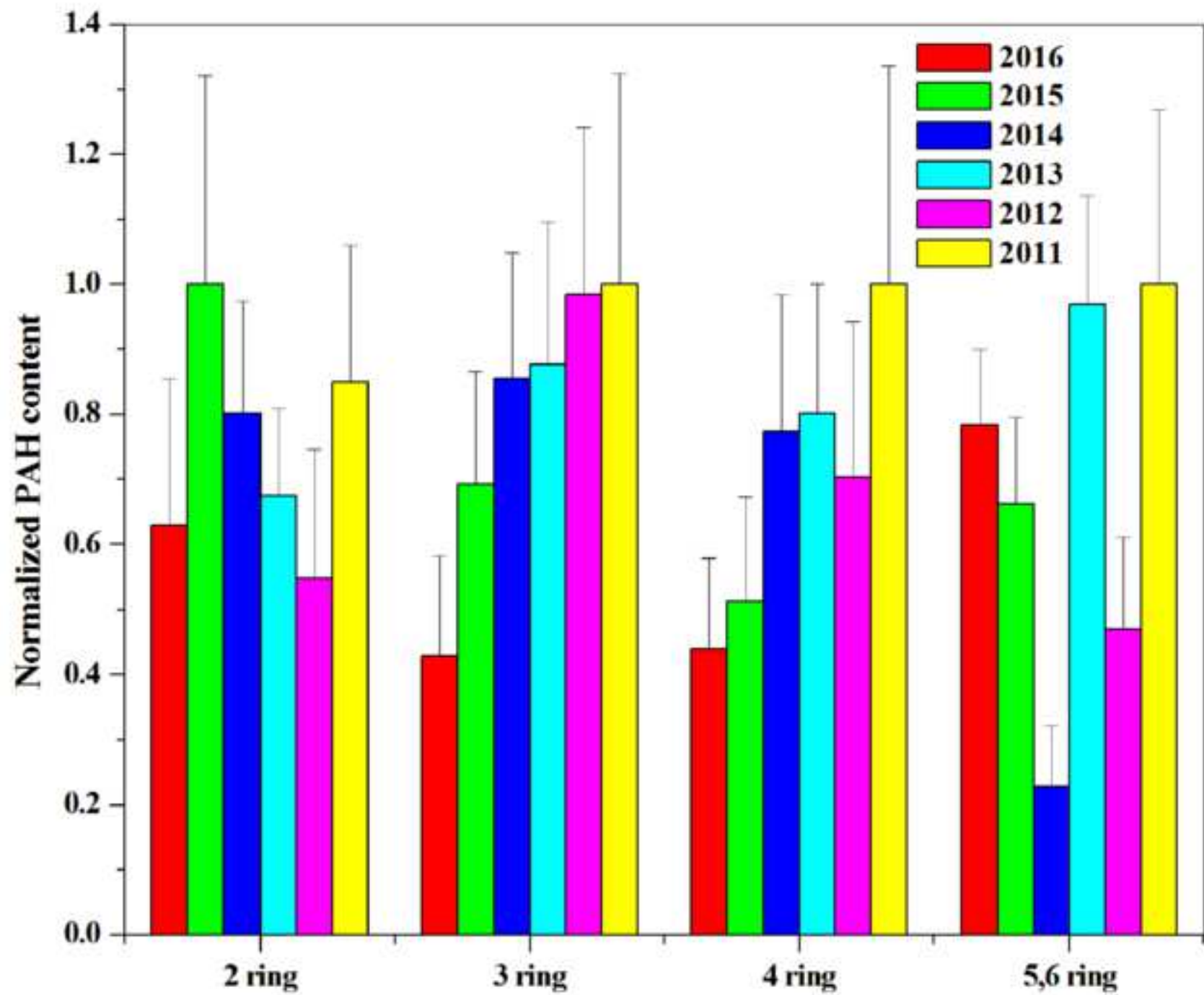


Figure 3
[Click here to download high resolution image](#)

